

Training-Free Multi-Concept Image Editing

Niki Foteinopoulou¹ Ignas Budvytis² Stephan Liwicki¹

¹Cambridge Research Laboratory, Toshiba Europe

²Independent Researcher

{niki.foteinopoulou, stephan.liwicki}@toshiba.eu

ignas.budvytis@gmail.com

Abstract

Editing images with diffusion models without training remains challenging. While recent optimisation-based methods achieve strong zero-shot edits from text, they struggle to preserve identity or capture details that language alone cannot express. Many visual concepts such as facial structure, material texture, or object geometry are impossible to express purely through text prompts alone. To address this gap, we introduce a training-free framework for concept-based image editing, which unifies Optimised DDS with LoRA-driven concept composition, where the training data of the LoRA represent the concept. Our approach enables combining and controlling multiple visual concepts directly within the diffusion process, integrating semantic guidance from text with low-level cues from pretrained concept adapters. We further refine DDS for stability and controllability through ordered timesteps, regularisation, and negative-prompt guidance. Quantitative and qualitative results demonstrate consistent improvements over existing training-free diffusion editing methods on InstructPix2Pix and ComposLoRA benchmarks. Code will be made publicly available.

1. Introduction

Recent advances in conditional image generation have brought us remarkably close to human-level quality in both image creation and editing [19, 28, 29, 33]. This progress is largely driven by diffusion models trained on vast, diverse datasets [34, 40], which enable high-fidelity synthesis guided by flexible conditioning signals such as text, sketches, or images. Among these, text-to-image diffusion models have become particularly influential, thanks to their intuitive natural-language control, which often allows high-level control without requiring task-specific fine-tuning.

However, editing existing images poses a subtler challenge than generating them from scratch. Effective editing requires not only semantic understanding but also content

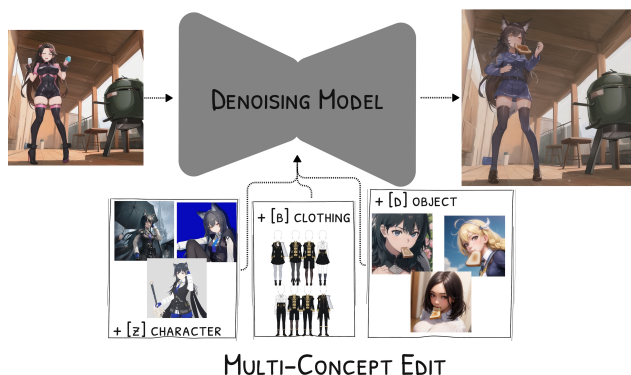
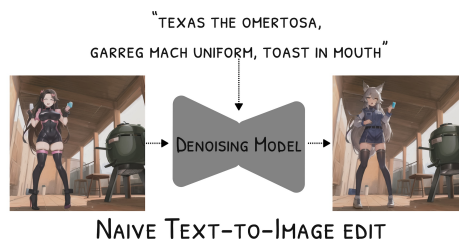


Figure 1. Our method enables training-free, concept-based image editing with diffusion models. By unifying an Optimised Delta Denoising Score (DDS) objective with LoRA-driven concept composition, we enable multiple visual concepts, such as facial structure, clothing, or objects, to be combined and controlled directly within the diffusion process that would be impossible to adequately describe in text alone. This approach preserves concept identity and fine-grained details while supporting complex edits, bridging the gap between text-based and visual concept-driven control.

consistency, ensuring that the edited image remains recognisably the same subject. Recent training-free optimisation-based methods such as DDS [8] achieve impressive zero-shot edits by refining the Score Distillation Sampling (SDS) objective [27], providing strong semantic control when an edit can be clearly expressed in natural language. Yet, language alone is an insufficient descriptor for all visual concepts. Many attributes defining identity, such as structure, texture, or object-specific geometry, exist below the level of

linguistic abstraction. As a result, DDS often fails when edits involve multiple entities or concept-specific features that cannot be captured purely by text prompts.

In parallel, personalisation methods such as Dream-Booth [31] and Low-Rank Adaptation (LoRA) [11] have demonstrated how instance-specific information can be encoded directly into a diffusion model’s parameters. LoRAs effectively serve as compact concept representations, embedding appearance, style, or identity traits that text cannot describe. However, current multi-LoRA composition techniques [6, 24, 41] are primarily designed for text-to-image generation, not for editing existing images where spatial alignment and subject consistency must be maintained.

This work unifies optimisation-based image editing and LoRA-based concept composition into a single framework for concept-aware, instance-consistent editing. DDS offers precise local control via optimisation, while LoRAs provide low-level, semantically grounded priors that anchor edits to specific concepts or instances. Combining the two enables edits that are both semantically meaningful and visually consistent across multiple concepts (Figure 1). Here, a concept denotes any coherent visual attribute encoded by a LoRA adapter that text alone cannot capture. Each LoRA thus serves as a reusable latent prior and low-level anchor within the optimisation loop (Figure 2), enabling controlled, consistent multi-concept editing.

While previous works have explored zero-shot editing [8, 17] or LoRA composition [6, 41], we contribute a unified training-free optimisation-based formulation that integrates both within a single inference-time loop, without retraining. The novelty lies in demonstrating that this integration yields stable, spatially aware, concept-preserving edits under the strict training-free constraint.

We first revisit DDS from both theoretical and practical perspectives, identifying key design factors that limit stability and edit fidelity. Through principled refinements – namely, timestep ordering, regularisation, and negative-prompt guidance – we derive a more stable and faithful Optimised DDS formulation. Building on this, we integrate a multi-LoRA composition mechanism directly into the optimisation loop, enabling spatially-aware, fine-grained, multi-concept editing without retraining or architectural changes. This mechanism performs patch-wise weighting of multiple LoRA outputs based on their feature similarity with the base model’s output, thereby producing the predicted noise for the optimised image.

Our contributions are summarised as follows:

- **Optimised DDS:** We introduce a refined delta-denoising formulation that improves stability, fidelity, and controllability in zero-shot image editing through ordered timesteps, regularisation, and negative-prompt guidance.
- **Concept-Preserving, Multi-Element Editing:** We propose the first unified framework that combines Optimised

DDS with composable LoRA adapters, enabling controllable, concept-level edits that preserve style, object or character low-level features.

- **Validation:** We demonstrate that our method generalises across diverse editing scenarios, from text-driven zero-shot edits to complex pose transformations and multi-element composition, achieving state-of-the-art results on InstructPix2Pix [1] and ComposLoRA [41].

2. Related Work

Diffusion-based Editing: Recent diffusion-based editing methods adapt text-to-image models for image modification by exploiting semantic priors. Approaches like Prompt-to-Prompt [25], Plug-and-Play, DiffEdit [3], and MasaCtrl [2] use attention manipulation, masking, or diffusion inversion for localised, text-guided edits, while Null-Text [25] inversion enhances reconstruction fidelity. However, their reliance on text conditioning often compromises instance preservation, especially for personalised or multi-concept edits. Optimisation-based methods such as SDS [27] align parametric representations with diffusion priors but can cause unwanted global changes. DDS [8] mitigates this via differential gradients, and PDS [17] adds regularisation to retain image composition (Sec. 3). Both randomly sample steps and remain confined to text-to-image edits. Our work extends these directions by optimising a DDS formulation that integrates ordered timesteps, posterior regularisation, and negative prompt guidance for more stable, concept-consistent, and composable edits also shown in Figure 4.

Composable Text-to-Image Generation seeks to synthesise images that coherently blend several user-defined concepts. Early work used structured conditioning—layouts or scene graphs—to improve compositionality [7, 15, 39]. Diffusion-based methods later refined the generative process or prompting to handle multi-concept inputs [5, 13, 18, 21, 26], but often depend on prompt design and struggle with rare or personalised elements. Modular systems [4, 20, 22, 37] combine separately trained models yet require heavy fine-tuning. We instead propose a training-free framework that composes LoRA adapters for spatially aware, fine-grained integration in image editing.

LoRA-Based Skill Composition. LoRA provides lightweight personalisation for large diffusion models [31, 38] in image generation. Approaches such as LoRAHub, ZipLoRA, and related mixture- or hypernetwork-based schemes [12, 32, 35, 36, 42] combine multiple LoRAs through learned weighting, but require supervision and offer limited generalisation. Arithmetic or attention-driven merging (LoRA Merge, CLoRA) [14, 24] and inference-time strategies (LoRA Switch, Composite, MultiLFG) [30, 41, 43] avoid retraining yet suffer from instability and inefficiency as LoRAs accumulate. LoRAtorio [6] proposes using the distance of LoRA-enhanced model predictions

from that of the base model as a measure of certainty, but does not use it for image editing. None of the multi-LoRA composition methods is implemented in image editing to demonstrate a concept-based generation that is controllable. To our knowledge, we are the first to formalise the multi-concept editing task and propose a method that addresses this.

3. Preliminaries

Score Distillation Sampling (SDS): Score Distillation Sampling (SDS) [27] leverages pretrained diffusion models to optimise a parametric image or 3D representation x_θ by matching the model’s predicted noise to that of a frozen teacher network $\epsilon_\theta(z_t, y)$ conditioned on a text prompt y . The SDS gradient can be written as

$$\nabla_\theta \mathcal{L}_{\text{SDS}} = \mathbb{E}_{t, \epsilon_t} \left[w(t) (\epsilon_\theta(z_t, y) - \epsilon_t) \frac{\partial z_0}{\partial \theta} \right], \quad (1)$$

where $w(t)$ is a time-dependent weighting term and z_t denotes the noisy latent corresponding to x_θ . The timesteps t are uniformly randomly sampled, ensuring denoising across varying noise magnitudes rather than following the forward diffusion order. Although SDS provides an effective means for optimising image parameters under text guidance, it often introduces undesired global updates when used for editing (Figure 4).

Delta Denoising Score (DDS): To mitigate the spurious gradients of SDS in image editing, Delta Denoising Score (DDS) [8] removes the source-conditioned denoising component from the target’s score estimate, leaving only the differential (“delta”) signal corresponding to the semantic change between prompts. The DDS gradient is given by:

$$\nabla_\theta \mathcal{L}_{\text{DDS}} = \mathbb{E}_{t, \epsilon_t} \left[w(t) (\epsilon_\theta(x_t^{\text{tgt}}, y_{\text{tgt}}, t) - \epsilon_\theta(x_t^{\text{src}}, y_{\text{src}}, t)) \frac{\partial x_0^{\text{tgt}}}{\partial \theta} \right], \quad (2)$$

where x_t^{src} and x_t^{tgt} denote the noised versions of the source and target latents, respectively, while y_{src} and y_{tgt} are their associated prompts. When the prompts coincide ($y_{\text{tgt}} = y_{\text{src}}$), the DDS gradient vanishes, thus preserving unedited regions. This formulation leads to more localised targeted edits with reduced blurring, although unintentional environment edits are not entirely eradicated.

Posterior Distillation Sampling (PDS): Building on the distillation framework, Posterior Distillation Sampling (PDS) [17] aligns posterior trajectories between source and target images, in practice introducing regularisation. Let x_t^{src} and x_t^{tgt} denote the latent trajectories obtained via stochastic diffusion inversion, and $\hat{\epsilon}_t^{\text{src}}, \hat{\epsilon}_t^{\text{tgt}}$ the corresponding predicted noises. The gradient is then:

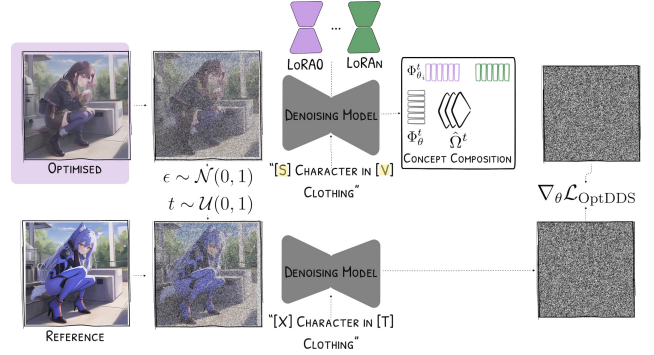


Figure 2. **Overview of our concept-based image editing framework.** We integrate multiple LoRA adapters into the Optimised DDS loop, enabling spatially-aware, concept-preserving edits across multiple concepts. The denoising trajectory follows ordered timesteps, allowing precise control over pose, style, and semantic attributes while maintaining overall composition.

$$\nabla_\theta \mathcal{L}_{\text{PDS}} = \mathbb{E}_{t, \epsilon_t, \epsilon_{t-1}} \left[\psi(t) (x_0^{\text{tgt}} - x_0^{\text{src}}) + \chi(t) (\hat{\epsilon}_t^{\text{tgt}} - \hat{\epsilon}_t^{\text{src}}) \right] \frac{\partial x_0^{\text{tgt}}}{\partial \theta} \quad (3)$$

where $\psi(t)$ and $\chi(t)$ are time-dependent weighting functions derived from the cumulative product of the variance schedule coefficients, used to balance the regularisation term $x_0^{\text{tgt}} - x_0^{\text{src}}$. However, as shown in [17], both $\psi(t)$ and $\chi(t)$ become zero with consequent timesteps, which we directly address in Sec. 4, and are dependent on the base model variance, not the intended edit.

4. Concept-Based Image Editing

In this section, we first formalise the problem of concept-based image editing and then propose a method to address this by first introducing an Optimised DDS formulation and then outlining our method for Composable Multi-LoRA integration. An overview can be seen in Figure 2.

Problem Formulation: We address the task of concept-based image editing in a zero-shot setting, where a pretrained text-to-image diffusion model serves as the generative prior. In our context, a concept refers to any semantically meaningful attribute that can be encoded via a LoRA adapter (e.g. such as a specific character) but cannot exclusively be captured by natural language. Each concept is assumed to be independently learnable and composable. Given a source image x_{src} and a set of editing conditions represented by a target prompt y^{tgt} , the objective is to synthesise a target image x_{tgt} that preserves the structural and concept attributes of x_{src} while incorporating the modifications specified by y^{tgt} .

Following the standard diffusion formulation, the forward process gradually perturbs a clean image x_0 with

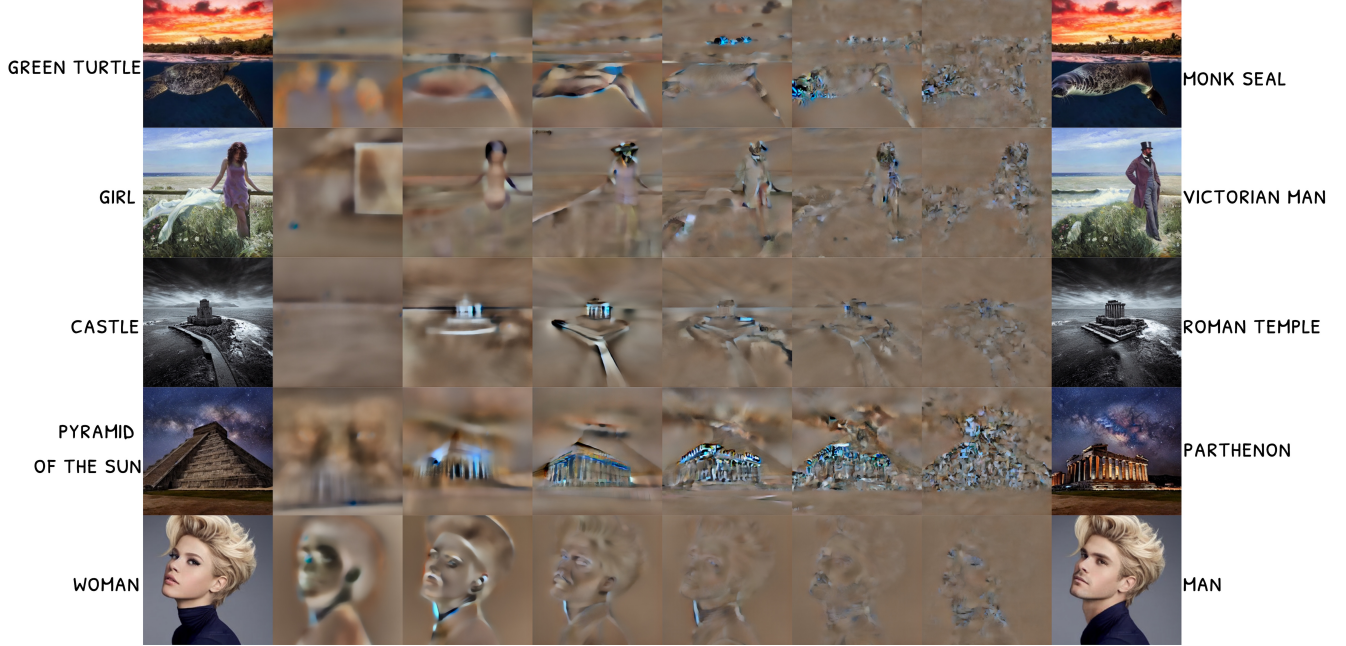


Figure 3. **Visualisation of timestep-ordered denoising.** Comparison between the source image, $\nabla_{\theta} \mathcal{L}_{\text{OptDDS}}$ at intermediate optimisation steps, and the final target image. Unlike DDS [8], which samples timesteps uniformly at random, our method enforces a strict descending timestep order, enabling a coarse-to-fine denoising trajectory as is evident from the visualised gradients. Early steps capture high-frequency structural details such as edges, while later steps refine lower-frequency and stylistic components, resulting in a more coherent and stable edit.

Gaussian noise:

$$x_t = \sqrt{\bar{\alpha}_t} x_0 + \sqrt{1 - \bar{\alpha}_t} \epsilon_t, \quad \epsilon_t \sim \mathcal{N}(0, I), \quad (4)$$

where $\bar{\alpha}_t = \prod_{s=1}^t \alpha_s$ denotes the cumulative product of variance schedule coefficients.

In the context of image editing, we define two latent trajectories corresponding to the source and target images :

$$\begin{aligned} x_t^{\text{src}} &= \sqrt{\bar{\alpha}_t} x_0^{\text{src}} + \sqrt{1 - \bar{\alpha}_t} \epsilon_t, \\ x_t^{\text{tgt}} &= \sqrt{\bar{\alpha}_t} x_0^{\text{tgt}} + \sqrt{1 - \bar{\alpha}_t} \epsilon_t, \end{aligned} \quad (5)$$

where x_0^{tgt} denotes the parametric representation of the target image to be optimised.

The objective of editing is to update the parameters of x_0^{tgt} such that the change in predicted noise between the source and target trajectories reflects visual modification:

$$\epsilon_{\theta_j}(x_t^{\text{tgt}}, y^{\text{tgt}}, t) - \epsilon_{\theta_j}(x_t^{\text{src}}, y^{\text{src}}, t) \approx x_0^{\text{tgt}} - x_0^{\text{src}}, \quad (6)$$

as specified by the editing conditions encoded in y^{tgt} .

To enable fine-grained and composable edits, we assume that the denoising network ϵ_{θ} can be parameterised with multiple LoRA modules, $\{\theta_1, \theta_2, \dots, \theta_N\}$, each encoding a distinct concept (e.g., a style, object, or attribute). The corresponding noise estimates are defined as:

$$\epsilon_{\theta_i}(x_t, y, t), \quad i = 1, \dots, N, \quad (7)$$

where each θ_i modulates the LoRA-enhanced diffusion model to represent a specific concept.

Our aim is thus to find an optimal x_0^{tgt} that yields edits faithful to the source image x^{src} while leveraging the personalised representations encoded by the LoRA parameters $\{\theta_i\}$ and avoiding concept clashes that emerge from the composition of multiple LoRAs.

Optimised DDS: We revisit the Delta Denoising Score (DDS) formulation and propose an enhanced variant, Optimised DDS, as it is the basis of the concept-based image editing pipeline. We first introduce an ordered-timestep strategy to improve the structure refinement during denoising. We then reformulate the regularisation term of PDS [17] so that the gradient does not vanish with ordered timesteps. Finally, we integrate negative prompts to improve image quality and semantic coherence further.

DDS [8] computes gradients by averaging over randomly sampled, non-sequential timesteps $t \sim \mathcal{U}(0, 1)$. This stochastic sampling ensures generalisation; however, it disregards the intrinsic temporal structure of the diffusion process observed in prior works [10, 30, 43], where early denoising steps predominantly reconstruct high-frequency and structural components such as edges, while later steps refine low-frequency and stylistic features. To exploit this property, we introduce a strict timestep ordering strategy, where the timesteps are sorted in descending order $1 >$

$u > \dots > v > 0$, where $u, v \sim \mathcal{U}(0, 1)$ during the optimisation process, ensuring a coarse-to-fine denoising progression, shown in Figure 3.

The ordering of timesteps introduces more unintended changes in the edited image, for which we introduce a regularisation objective similar to PDS, so that:

$$\nabla_{\theta} \mathcal{L}_{\text{OptDDS}} = \mathbb{E}_{t, \epsilon_t, \epsilon_{t-1}} \left[(\eta |x_0^{\text{tgt}} - x_0^{\text{src}}| + (\hat{\epsilon}_t^{\text{tgt}} - \hat{\epsilon}_t^{\text{src}})) \frac{\partial x_0^{\text{tgt}}}{\partial \theta} \right], \quad (8)$$

where $\hat{\epsilon}_t^{\text{src}}$ and $\hat{\epsilon}_t^{\text{tgt}}$ are the predicted noise terms for the source and target, respectively, and η is a hyperparameter controlling the relative strength of latent alignment. This formulation leads to improved concept preservation and smoother transitions between editing stages (Figure 3), while maintaining generalisation compared to baseline Equation (2), further explored in Sec. 5.4. The simple formulation is more robust and intentionally controlled than Equation (3), as it allows for inference with all formulations, including ordering timesteps where Equation (3) becomes zero.

Finally, we incorporate negative prompts into the DDS optimisation process. Given a positive prompt y^+ and a negative prompt y^- , we define the guided noise prediction:

$$\hat{\epsilon}(z_t, y^+, t) = (1 + \lambda)\epsilon(z_t, y^+, t) - \lambda\epsilon(z_t, y^-, t) \quad (9)$$

where λ controls the strength of classifier-free guidance [9]. By including negative prompts (e.g., “blurry”, “distorted”, “low quality”) during the conditioning of ϵ_{θ} , the denoising process becomes biased against degenerate visual modes, thus improving qualitative output.

Ordered timesteps encourage a coarse-to-fine optimisation trajectory that mirrors the natural denoising process, stabilising gradients that would otherwise oscillate under uniform sampling. The regularisation coefficient η balances edit strength and structural preservation: a larger η enforces a stronger latent alignment at the cost of edit intensity. The classifier-free guidance weight λ controls the suppression of unwanted artefacts, while the patch-temperature τ adjusts spatial selectivity during multi-LoRA fusion.

Composable Multi-LoRA Integration for Concept-Based Image Editing: A key limitation of diffusion-based editing methods is their reliance on text prompts, which often fail to preserve subject fidelity across pose or style changes. Approaches [8] leveraging DreamBooth’s [31] concept-specific adapters partially address this by enabling more controlled single-concept edits, yet extending to multi-concept or compositional edits remains an open challenge.

To enable multi-concept editing, we use the patchwise similarity of the LoRA predictions from the base model as a

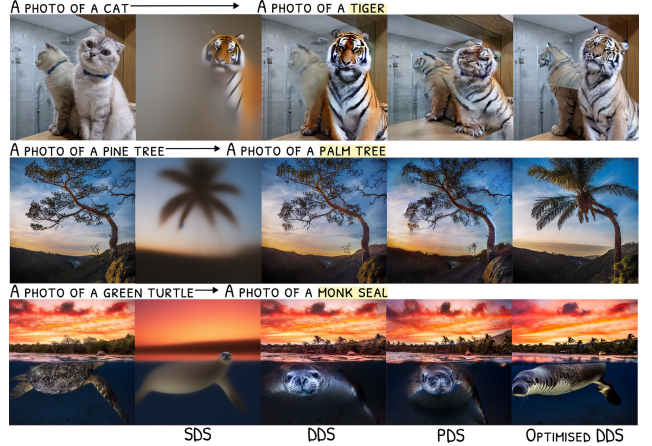


Figure 4. Comparison of our Optimised DDS vs baselines. Our method produces better results for the target subject with similarly perceived changes in the background.

proxy for confidence [6]. Let $e_{\theta_i}(z_t, t, c)$ denote the prediction of the i^{th} LoRA. We first spatially tokenise the output of each LoRA, and the base model:

$$\Phi_{\theta}^t = \phi(e_{\theta}(z_t, t, c)), \quad \Phi_{\theta_i}^t = \phi(e_{\theta_i}(z_t, t, c)), \quad (10)$$

where ϕ flattens each $H \times W$ feature map into P patch vectors. We compute the cosine similarity between corresponding patches:

$$\Omega_i^t = \langle \Phi_{\theta}^t, \Phi_{\theta_i}^t \rangle_{\text{cos}}, \quad (11)$$

We apply a SoftMin, as high similarity with the base model implies low confidence of the LoRA adapters, with temperature τ to obtain patch-wise LoRA weights and upscale the Ω weights back to the original dimensions:

$$\hat{\Omega}_i^t = \text{softmax}_{\tau}(\Omega_i^t), \quad \hat{\Omega}_i^{t, \text{up}} = \hat{\Omega}_i^t \otimes \mathbf{1}_{d \times d}. \quad (12)$$

The final conditional noise prediction is computed as a weighted combination of all LoRA predicted noise:

$$\tilde{\epsilon}(z_t, t, c) = \sum_{i=1}^N \hat{\Omega}_i^{t, \text{up}} \epsilon_{\theta_i}(z_t, t, c). \quad (13)$$

This composition is applied at each denoising step during editing. By combining multiple LoRAs spatially, we can simultaneously preserve concepts and apply multiple semantic changes when integrated with Optimised DDS.

5. Results

5.1. Implementation Details

For a fair comparison with previous works, we select *stable-diffusion-v1.5* [29] as the backbone for all experiments.

For experiments on InstructPix2Pix, we select 1000 images from the train set for all zero-shot comparisons with DDS. We use a guidance scale $s = 10$, and image size 512×512 and checkpoint “runwayml/stable-diffusion-v1-5”. For our experiments in the MultiLoRA setting, we follow the setup of [41], using *ComposLoRA* tests that include 22 pre-trained LoRAs spanning characters, clothing, styles, backgrounds, and objects. We use the “Realistic_Vision_V5.1” and “Counterfeit-V2.5” checkpoints for realistic and anime-style images, respectively. For the realistic subset, a guidance scale $s = 7$, and image size 512×512 ; for the anime subset we use $s = 10$. DPM-Solver++ [23] is used as the sampler, with all LoRAs scaled by a weight of 0.8. We empirically set the temperature $\tau = 0.002$. For all experiments, we set the size of each patch to 2×2 . For all experiments, we select 300 denoising steps and set $\eta = 0.5$. Since our method operates at inference time, all experiments are run on a single RTX A6000 GPU. Results are averaged over three runs. We provide an extended sensitivity analysis of hyperparameters in Sec. 8.

5.2. Quantitative Evaluation of Image Editing

Optimised DDS: We evaluate our Optimised DDS method on the InstructPix2Pix benchmark in Tab. 1. Our method achieves a statistically significant improvement in CLIP-Score over previous SoTA at 99% confidence interval, while maintaining comparable LPIPS, visualised in Figure 4.

Table 1. **Quantitative Evaluation of our optimised DDS method against previous SoTA, on InstructPix2Pix.** Our method achieves statistically significant improvements in CLIP-Score while maintaining comparable LPIPS.

	CLIPScore \uparrow	LPIPS \downarrow
DiffusionClip \ddagger	0.251 \pm 0.022	0.572 \pm 0.0594
PnP \ddagger	0.221 \pm 0.036	0.310 \pm 0.075
InstructPix2Pix \ddagger	0.219 \pm 0.037	0.322 \pm 0.215
DDS \ddagger	0.225 \pm 0.031	0.104 \pm 0.061
PDS \ddagger	0.298 \pm 0.044	0.096 \pm 0.033
Optimised DDS	0.308 \pm 0.042*	0.100 \pm 0.042

\ddagger Reported in [8]

\ddagger Adaptation of algorithm presented in [17] for RGB images

* statistically significant at 99% confidence interval.

Concept-Based Edit: To evaluate the effectiveness of our method in multi-concept editing, we integrate Optimised DDS with the proposed LoRA composition framework and compare it against three existing strategies: *Composite* [41], *Switch* [41], and *Merge* [14], selected as they have publicly available code that can be adopted to image editing, without multiple inference steps. For each configuration, we generate scenes containing N distinct LoRAs, each representing a different concept from the *ComposLoRA* testbed

(character, clothing, object, background or style). We then apply our method to simultaneously edit all N entities into different but semantically consistent counterparts (e.g., $\text{character}_1 \rightarrow \text{character}_2$, $\text{clothing}_1 \rightarrow \text{clothing}_2$). This process is repeated across all valid concept combinations in the testbed to ensure a comprehensive evaluation of both cross-concept consistency and edit controllability.

In Tab. 2, our method achieves the lowest LPIPS across nearly all configurations, indicating stronger concept preservation and spatial consistency. CLIPScore remains on par or higher than baselines but saturates with more concepts, likely due to modality gaps and prompt ambiguity, suggesting that alone it’s insufficient to capture perceptual and compositional quality in multi-concept edits. We see, however, that all methods have CLIPScores in similar ranges, which indicates that CLIPScore is adequate to measure whether the generic object is included, but not if the specific concept and instance are represented, thus highlighting the need for qualitative evaluation.

5.3. Qualitative Evaluation via GPT-4V and Human Ranking

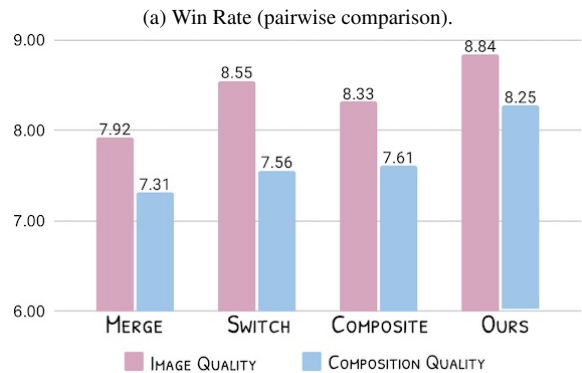
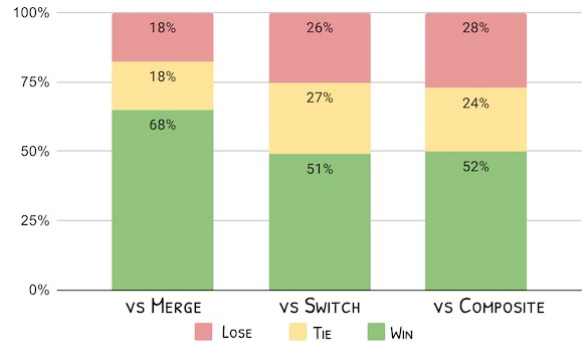


Figure 5. **Comparison of our Optimised DDS with concept composition against previous LoRA-composition methods, evaluated using GPT-4V.** Our method achieves higher perceived image and composition quality, with consistently higher pairwise win rates.

Since CLIPScore alone cannot capture compositional

Table 2. **Quantitative Evaluation of Optimised DDS + Multi-LoRA Composition.**

Performance comparison across four LoRA composition strategies for different numbers of LoRAs on *ComposLoRA* testbed. **Bold** values indicate statistical significance at the 99% confidence interval.

	$N = 2$		$N = 3$		$N = 4$		$N = 5$		Total	
	CLIPScore \uparrow	LPIPS \downarrow								
Ours	0.340 \pm 0.030	0.401 \pm 0.174	0.361 \pm 0.022	0.461 \pm 0.158	0.370 \pm 0.019	0.534 \pm 0.104	0.368 \pm 0.059	0.503 \pm 0.082	0.359 \pm 0.032	0.474 \pm 0.129
Composite	0.351 \pm 0.021	0.542 \pm 0.150	0.369 \pm 0.019	0.613 \pm 0.129	0.377 \pm 0.018	0.644 \pm 0.077	0.363 \pm 0.057	0.664 \pm 0.039	0.365 \pm 0.028	0.615 \pm 0.098
Switch	0.350 \pm 0.021	0.456 \pm 0.145	0.361 \pm 0.021	0.485 \pm 0.147	0.367 \pm 0.020	0.467 \pm 0.128	0.363 \pm 0.057	0.487 \pm 0.108	0.360 \pm 0.029	0.473 \pm 0.132
Merge	0.346 \pm 0.016	0.547 \pm 0.133	0.352 \pm 0.018	0.601 \pm 0.112	0.354 \pm 0.021	0.634 \pm 0.067	0.346 \pm 0.061	0.662 \pm 0.038	0.349 \pm 0.029	0.610 \pm 0.087

(a) Reality

	$N = 2$		$N = 3$		$N = 4$		$N = 5$		Total	
	CLIPScore \uparrow	LPIPS \downarrow	CLIPScore \uparrow	LPIPS \downarrow	CLIPScore \uparrow	LPIPS \downarrow	CLIPScore \uparrow	LPIPS \downarrow	CLIPScore \uparrow	LPIPS \downarrow
Ours	0.324 \pm 0.026	0.321 \pm 0.096	0.327 \pm 0.027	0.313 \pm 0.084	0.331 \pm 0.027	0.314 \pm 0.079	0.318 \pm 0.029	0.306 \pm 0.067	0.325 \pm 0.027	0.314 \pm 0.082
Composite	0.324 \pm 0.029	0.658 \pm 0.057	0.320 \pm 0.031	0.67 \pm 0.068	0.327 \pm 0.026	0.668 \pm 0.058	0.310 \pm 0.022	0.663 \pm 0.039	0.320 \pm 0.027	0.665 \pm 0.055
Switch	0.331 \pm 0.028	0.378 \pm 0.07	0.335 \pm 0.03	0.368 \pm 0.053	0.339 \pm 0.025	0.316 \pm 0.047	0.331 \pm 0.024	0.319 \pm 0.043	0.334 \pm 0.027	0.345 \pm 0.053
Merge	0.341 \pm 0.026	0.388 \pm 0.091	0.341 \pm 0.03	0.428 \pm 0.091	0.340 \pm 0.026	0.473 \pm 0.094	0.331 \pm 0.022	0.498 \pm 0.084	0.338 \pm 0.026	0.447 \pm 0.090

(b) Anime

Table 3. **Human evaluation comparing our Optimised DDS with concept composition to previous LoRA-composition methods.** In line with GPT-4V assessments, human raters consistently preferred our method, which achieved the lowest average rank and most frequent first-place selections (highest win rate).

	Avg. Rank \downarrow	Win Rate \uparrow
Ours	1.90	38%
Compose	2.62	31%
Switch	2.49	25%
Merge	3.00	5%

quality, we complement it with qualitative evaluations using GPT-4V and human studies. Examples can be seen in Sec. 9. GPT-4V scores and pairwise win rates against Switch, Composite, and Merge are shown in Figure 5b and Figure 5a. Human evaluators likewise ranked our method highest for image quality and concept integration, with the lowest average rank in Tab. 3, followed closely by Switch. Additional results can be seen in Sec. 9.



Figure 6. **Samples generated from the base model using text descriptions.** We observe distortions in the face, additional limbs, missing concepts, and inconsistent knowledge of characters and objects, all of which affect downstream tasks.

Table 4. **Optimised DDS Ablation.** We use baseline DDS with 300 steps (unless otherwise indicated), and add individual components to isolate the effect of each change ceteris paribus. Our method finds a balance between conceptual changes and maintaining image structure.

	CLIPScore \uparrow	LPIPS \downarrow
DDS (200 steps)	0.225 \pm 0.031	0.104 \pm 0.061
DDS	0.305 \pm 0.039	0.264 \pm 0.061
DDS+Strict Timesteps	0.332 \pm 0.032	0.461 \pm 0.076
DDS+Regularisation	0.291 \pm 0.041	0.081 \pm 0.033
DDS+Neg.Prompts	0.318 \pm 0.040	0.319 \pm 0.076
Optimised DDS	0.308 \pm 0.042	0.100 \pm 0.042

5.4. Ablation

As shown in Tab. 4, enforcing ordered timesteps increases both metrics, reflecting stronger structural changes consistent with more pronounced edits. In contrast, adding regularisation lowers both metrics, indicating overly conservative optimisation that can suppress edits entirely. Balancing these two effects produces the best trade-off between edit strength and perceptual fidelity, along visual inspection. Additional ablations on the effect of chosen hyperparameters can be seen in Sec. 8.

5.5. Pose Changes Under Concept Preservation

By integrating multiple LoRA adapters into the Optimised DDS framework, our method extends DDS’s capabilities to support edits involving pose and semantic changes. As shown in Figure 7, it maintains subject fidelity across pose and expression variations while preserving key compositional features in multi-LoRA edits.

6. Limitations and Error Analysis

Despite its training-free design, our method incurs non-negligible computational cost. Runtime increases approx-

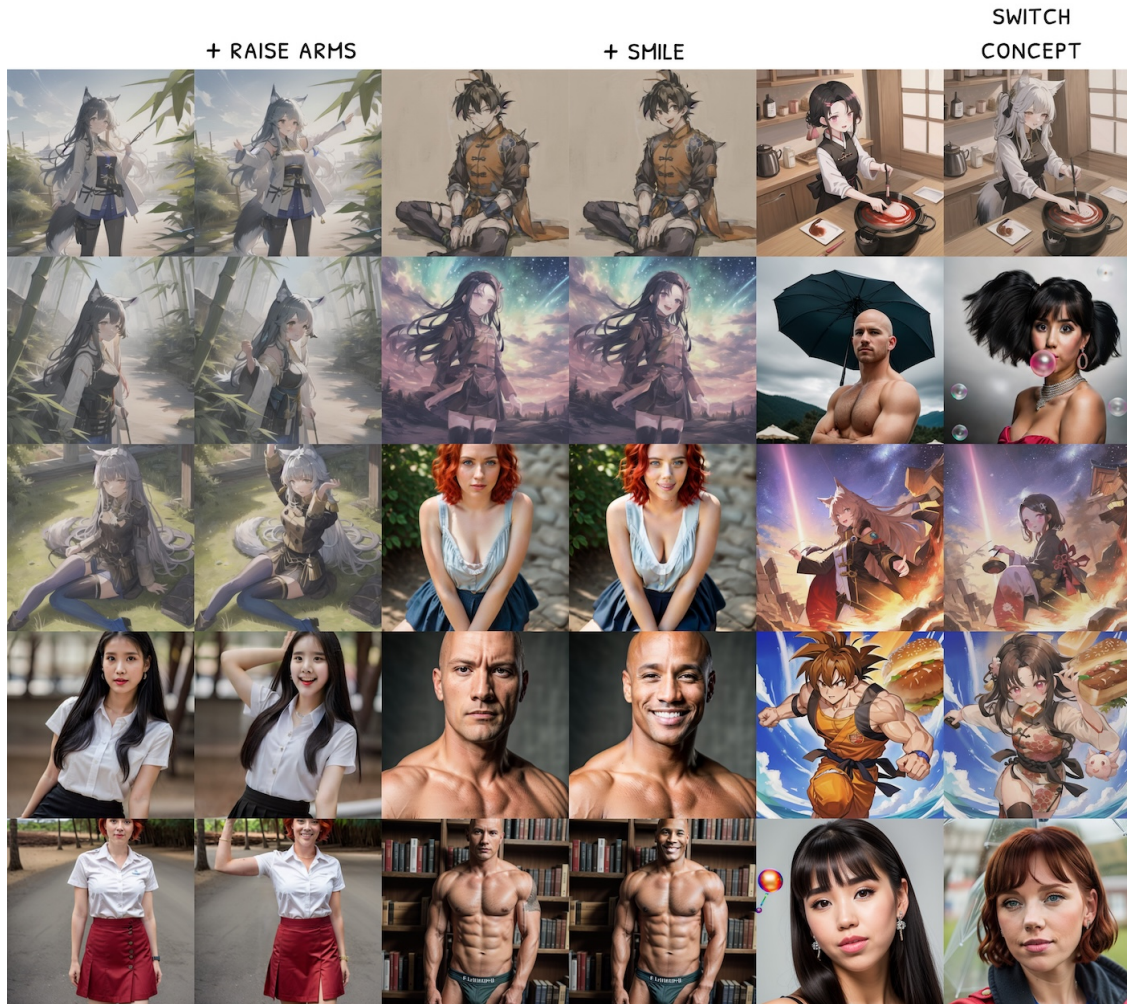


Figure 7. **Examples of our method under different editing conditions.** Our approach enables consistent and coherent edits across diverse scenarios, including pose changes, facial expression modifications, and element or object swaps (*e.g.*, between different characters and environmental components). Each pair demonstrates the method’s ability to preserve subject and visual fidelity while adapting to the intended transformation.

imately linearly with the number of LoRA adapters, as each adapter contributes a separate noise prediction. On an RTX A6000, a 512×512 edit with five LoRAs requires 44s compared to 27s for a text-to-image edit with Optimised DDS. While feasible for offline editing, this limits interactive use. Performance also depends on the quality and mutual alignment of LoRA adapters. Variability in publicly available LoRAs (*e.g.*, inconsistent training data or rank) can introduce imbalance, occasionally biasing the composite output toward dominant adapters. Finally, generation quality remains bounded by the base model: artefacts such as duplicated limbs or entangled concepts (*e.g.*, prompts such as “raise arm” that also cause a smile) stem from the base model’s inherent priors, and are not explicitly addressed by our method(Figure 6).

7. Conclusion

We present a unified framework for controllable, concept-based image editing by first optimising DDS, and then combining the Optimised DDS with multi-LoRA composition. Our method enables fine-grained, multi-concept edits without retraining, maintaining subject fidelity even under complex transformations, such as changes of multiple conceptual elements. Extensive quantitative and qualitative evaluations demonstrate state-of-the-art performance across both single and multi-concept edits.

References

- [1] Tim Brooks, Aleksander Holynski, and Alexei A Efros. Instructpix2pix: Learning to follow image editing instructions.

- arXiv preprint arXiv:2211.09800*, 2022. 2, 1
- [2] Mingdeng Cao, Xintao Wang, Zhongang Qi, Ying Shan, Xiaohu Qie, and Yinqiang Zheng. Masactrl: Tuning-free mutual self-attention control for consistent image synthesis and editing. In *Proceedings of the IEEE/CVF international conference on computer vision*, pages 22560–22570, 2023. 2
 - [3] Guillaume Couairon, Jakob Verbeek, Holger Schwenk, and Matthieu Cord. Diffedit: Diffusion-based semantic image editing with mask guidance. *arXiv preprint arXiv:2210.11427*, 2022. 2
 - [4] Yilun Du, Shuang Li, and Igor Mordatch. Compositional visual generation with energy based models. *Advances in Neural Information Processing Systems*, 33:6637–6647, 2020. 2
 - [5] Weixi Feng, Xuehai He, Tsu-Jui Fu, Varun Jampani, Arjun Reddy Akula, Pradyumna Narayana, Sugato Basu, Xin Eric Wang, and William Yang Wang. Training-free structured diffusion guidance for compositional text-to-image synthesis. In *The Eleventh International Conference on Learning Representations*, 2023. 2
 - [6] Niki Foteinopoulou, Ignas Budvytis, and Stephan Liwicki. Loratorio: An intrinsic approach to lora skill composition, 2025. 2, 5
 - [7] Oran Gafni, Adam Polyak, Oron Ashual, Shelly Sheynin, Devi Parikh, and Yaniv Taigman. Make-a-scene: Scene-based text-to-image generation with human priors. In *European Conference on Computer Vision*, pages 89–106. Springer, 2022. 2
 - [8] Amir Hertz, Kfir Aberman, and Daniel Cohen-Or. Delta denoising score. In *Proceedings of the IEEE/CVF International Conference on Computer Vision (ICCV)*, pages 2328–2337, 2023. 1, 2, 3, 4, 5, 6
 - [9] Jonathan Ho and Tim Salimans. Classifier-free diffusion guidance. In *NeurIPS 2021 Workshop on Deep Generative Models and Downstream Applications*, 2021. 5
 - [10] Jonathan Ho, Ajay Jain, and Pieter Abbeel. Denoising diffusion probabilistic models. *Advances in neural information processing systems*, 33:6840–6851, 2020. 4
 - [11] Edward J Hu, Yelong Shen, Phillip Wallis, Zeyuan Allen-Zhu, Yuanzhi Li, Shean Wang, Lu Wang, Weizhu Chen, et al. Lora: Low-rank adaptation of large language models. *ICLR*, 1(2):3, 2022. 2
 - [12] Chengsong Huang, Qian Liu, Bill Yuchen Lin, Tianyu Pang, Chao Du, and Min Lin. Lorahub: Efficient cross-task generalization via dynamic lora composition. In *Conference on Language Modeling*, 2024. 2
 - [13] Lianghua Huang, Di Chen, Yu Liu, Yujun Shen, Deli Zhao, and Jingren Zhou. Composer: creative and controllable image synthesis with composable conditions. In *Proceedings of the 40th International Conference on Machine Learning*. JMLR.org, 2023. 2
 - [14] Hugging Face. Merging loras. https://huggingface.co/docs/diffusers/en/using-diffusers/merge_loras, 2024. Accessed: 2025-06-09. 2, 6
 - [15] Justin Johnson, Agrim Gupta, and Li Fei-Fei. Image generation from scene graphs. In *Proceedings of the IEEE conference on computer vision and pattern recognition*, pages 1219–1228, 2018. 2
 - [16] Maurice G Kendall and B Babington Smith. The problem of m rankings. *The annals of mathematical statistics*, 10(3): 275–287, 1939. 5
 - [17] Juil Koo, Chanhoo Park, and Minhyuk Sung. Posterior distillation sampling. In *CVPR*, 2024. 2, 3, 4, 6
 - [18] Nupur Kumari, Bingliang Zhang, Richard Zhang, Eli Shechtman, and Jun-Yan Zhu. Multi-concept customization of text-to-image diffusion. In *Proceedings of the IEEE/CVF conference on computer vision and pattern recognition*, pages 1931–1941, 2023. 2
 - [19] Black Forest Labs, Stephen Batifol, Andreas Blattmann, Frederic Boesel, Saksham Consul, Cyril Diagne, Tim Dockhorn, Jack English, Zion English, Patrick Esser, Sumith Kulal, Kyle Lacey, Yam Levi, Cheng Li, Dominik Lorenz, Jonas Müller, Dustin Podell, Robin Rombach, Harry Saini, Axel Sauer, and Luke Smith. Flux.1 kontext: Flow matching for in-context image generation and editing in latent space, 2025. 1
 - [20] Shuang Li, Yilun Du, Joshua B. Tenenbaum, Antonio Torralba, and Igor Mordatch. Composing ensembles of pre-trained models via iterative consensus. In *The Eleventh International Conference on Learning Representations*, 2023. 2
 - [21] Kevin Lin, Zhengyuan Yang, Linjie Li, Jianfeng Wang, and Lijuan Wang. Designbench: Exploring and benchmarking dall-e 3 for imagining visual design. *arXiv preprint arXiv:2310.15144*, 2023. 2
 - [22] Nan Liu, Shuang Li, Yilun Du, Josh Tenenbaum, and Antonio Torralba. Learning to compose visual relations. *Advances in Neural Information Processing Systems*, 34: 23166–23178, 2021. 2
 - [23] Cheng Lu, Yuhao Zhou, Fan Bao, Jianfei Chen, Chongxuan Li, and Jun Zhu. Dpm-solver++: Fast solver for guided sampling of diffusion probabilistic models. *arXiv preprint arXiv:2211.01095*, 2022. 6
 - [24] Tuna Han Salih Meral, Enis Simsar, Federico Tombari, and Pinar Yanardag. Clora: A contrastive approach to compose multiple lora models, 2024. 2
 - [25] Ron Mokady, Amir Hertz, Kfir Aberman, Yael Pritch, and Daniel Cohen-Or. Null-text inversion for editing real images using guided diffusion models. *arXiv preprint arXiv:2211.09794*, 2022. 2
 - [26] Ziheng Ouyang, Zhen Li, and Qibin Hou. K-lora: Unlocking training-free fusion of any subject and style loras. *arXiv preprint arXiv:2502.18461*, 2025. 2
 - [27] Ben Poole, Ajay Jain, Jonathan T Barron, and Ben Mildenhall. Dreamfusion: Text-to-3d using 2d diffusion. In *International Conference on Learning Representations*, 2023. 1, 2, 3
 - [28] Aditya Ramesh, Prafulla Pavlov, Gabriel Goh, Scott Gray, Chelsea Voss, Alec Radford, Mark Chen, and Ilya Sutskever. Hierarchical text-conditional image generation with clip latents (dall-e 2). In *arXiv preprint arXiv:2204.06125*, 2022. 1
 - [29] Robin Rombach, Andreas Blattmann, Dominik Lorenz, Patrick Esser, and Björn Ommer. High-resolution image synthesis with latent diffusion models. In *Proceedings of*

- the IEEE/CVF Conference on Computer Vision and Pattern Recognition*, pages 10684–10695, 2022. 1, 5
- [30] Aniket Roy, Maitreya Suin, Ketul Shah, and Rama Chellappa. Multlfg: Training-free multi-lora composition using frequency-domain guidance. *arXiv preprint arXiv:2505.20525*, 2025. 2, 4
- [31] Nataniel Ruiz, Yuanzhen Li, Varun Jampani, Yael Pritch, Michael Rubinstein, and Kfir Aberman. Dreambooth: Fine tuning text-to-image diffusion models for subject-driven generation. In *Proceedings of the IEEE/CVF Conference on Computer Vision and Pattern Recognition*, pages 22510–22510, 2023. 2, 5
- [32] Nataniel Ruiz, Yuanzhen Li, Varun Jampani, Wei Wei, Tingbo Hou, Yael Pritch, Neal Wadhwa, Michael Rubinstein, and Kfir Aberman. Hyperdreambooth: Hypernetworks for fast personalization of text-to-image models. In *Proceedings of the IEEE/CVF conference on computer vision and pattern recognition*, pages 6527–6536, 2024. 2
- [33] Chitwan Saharia, William Chan, Saurabh Saxena, Lala Li, Jay Whang, Emily Denton, Kelvin Ghasemipour, et al. Photorealistic text-to-image diffusion models with deep language understanding. In *Advances in Neural Information Processing Systems (NeurIPS)*, 2022. 1
- [34] Christoph Schuhmann, Romain Beaumont, Radu Vencu, Cade Gordon, Ross Wightman, Mehdi Cherti, Theo Coombes, Ashish Katta, Charlie Mullis, Mitchell Wortsman, Patrick Schramowski, Katherine Crowson, Ludwig Schmidt, Robin Kaczmarczyk, and Jenia Jitsev. Laion-5b: An open large-scale dataset for training next generation image-text models. *arXiv preprint arXiv:2210.08402*, 2022. 1
- [35] Viraj Shah, Nataniel Ruiz, Forrester Cole, Erika Lu, Svetlana Lazebnik, Yuanzhen Li, and Varun Jampani. Ziplora: Any subject in any style by effectively merging loras. In *European Conference on Computer Vision*, pages 422–438. Springer, 2024. 2
- [36] Donald Shenaj, Ondrej Bohdal, Mete Ozay, Pietro Zanuttigh, and Umberto Michieli. LoRA.rar: Learning to Merge LoRAs via Hypernetworks for Subject-Style Conditioned Image Generation, 2024. arXiv:2412.05148 [cs]. 2
- [37] Enis Simsar, Thomas Hofmann, Federico Tombari, and Pinar Yanardag. Loraclr: Contrastive adaptation for customization of diffusion models. In *Proceedings of the Computer Vision and Pattern Recognition Conference*, pages 13189–13198, 2025. 2
- [38] Kihyuk Sohn, Nataniel Ruiz, Kimin Lee, Daniel Castro Chin, Irina Blok, Huiwen Chang, Jarred Barber, Lu Jiang, Glenn Entis, Yuanzhen Li, et al. Styledrop: text-to-image generation in any style. In *Proceedings of the 37th International Conference on Neural Information Processing Systems*, pages 66860–66889, 2023. 2
- [39] Yang Song, Jascha Sohl-Dickstein, Diederik P Kingma, Abhishek Kumar, Stefano Ermon, and Ben Poole. Score-based generative modeling through stochastic differential equations. In *International Conference on Learning Representations*, 2021. 2
- [40] Shaoxiong Wang, Yang Yu, Ziqi Zhang, Yuxiang Zhang, Lizhou Cui, Zhihong Jiang, Yihan Wang, Yuting Guo, Zhenbang Zhang, Han Zhang, Yihong Gao, Kaiwen Liang, Wayne Xin Zhao, and Ji-Rong Wen. Diffusiondb: A large-scale prompt gallery dataset for text-to-image generative models. *arXiv preprint arXiv:2210.14896*, 2022. 1
- [41] Ming Zhong, Shuohang Wang, Yadong Lu, Yizhu Jiao, Siru Ouyang, Donghan Yu, Jiawei Han, Weizhu Chen, et al. Multi-lora composition for image generation. In *Transactions on Machine Learning Research*, 2024. 2, 6
- [42] Jie Zhu, Yixiong Chen, Mingyu Ding, Ping Luo, Leye Wang, and Jingdong Wang. MoLE: Enhancing Human-centric Text-to-image Diffusion via Mixture of Low-rank Experts. In *Advances in Neural Information Processing Systems*, pages 29354–29386. Curran Associates, Inc., 2024. 2
- [43] Xiandong Zou, Mingzhu Shen, Christos-Savvas Bouganis, and Yiren Zhao. Cached multi-lora composition for multi-concept image generation. In *13th International Conference on Learning Representations*, 2025. 2, 4

Training-Free Multi-Concept Image Editing

Supplementary Material

Table 5. Sensitivity of Optimised DDS to η hyperparameter, on InstructPix2pix.

η	CLIP \uparrow	LPIPS \downarrow
0.01	0.316 ± 0.040	0.407 ± 0.151
0.05	0.308 ± 0.042	0.100 ± 0.042
1	0.304 ± 0.042	0.090 ± 0.047
5	0.299 ± 0.044	0.079 ± 0.034
10	0.299 ± 0.044	0.089 ± 0.035

8. Sensitivity Analysis

We conduct a sensitivity analysis of our method to the key hyper-parameters defined in Sec. 4. For η , we evaluate our Optimised DDS on 1000 random images from the InstructPix2Pix[1] dataset, to allow for a fair comparison with baseline DDS. For patch size and sensitivity to temperature, we evaluate our method on the $N = 2 - 3$ anime subset of the ComposeLoRA testbed.

8.1. Sensitivity to Regularisation

We evaluate the effect of the hyperparameter η on the performance of Optimised DDS. Tab. 5 reports CLIP and LPIPS scores across a wide range of η values. Overall, we see that these metrics have an inverse relationship with a high ClipScore indicating high target semantic alignment and very low LPIPS indicating no change at all. Figure 8 further illustrates qualitative changes, showing that large η values do not negatively affect the edit when targeted edit area is small (e.g. “add smile”), but prevent edits of larger areas (e.g. “pine tree \rightarrow palm tree”). As such, the strength of the regularisation is highly dependent on the area of the edit with larger edits requiring a lower η and smaller target areas being robust with strong regularisation. We argue, that as the regularisation is dependent on the area of the edit and not the model used, a simpler user guided approach may offer more control to image editing.

8.2. Sensitivity to Patch Size

We further assess how patch size affects performance using a subset of the ComposeLoRA test bed. Patch size controls the granularity of local alignment, potentially impacting the method’s ability to capture and preserve compositional structure. Tab. 6 shows that smaller patches generally yield better CLIP scores, suggesting that finer local conditioning improves concept inclusion.



Figure 8. Sensitivity of Optimised DDS to η . When the change is smaller, the method is robust to large η values.

Table 6. Effect of patch size on a subset of the ComposeLoRA testbed. Although the method is relatively robust to patch size, the more localised approach shows higher ClipScore.

	$N = 2$	$N = 3$	Avg.
2×2	0.340 ± 0.030	0.361 ± 0.022	0.351
4×4	0.335 ± 0.029	0.356 ± 0.022	0.346
8×8	0.329 ± 0.031	0.349 ± 0.020	0.339
16×16	0.322 ± 0.029	0.341 ± 0.022	0.332

8.3. Sensitivity to temperature

Finally, we analyse the temperature parameter τ , which controls the sharpness of the probability distribution in the optimization process. Tab. 7 indicates that the method is robust to large changes in τ , as the performance does not collapse, but there is a clear improvement in terms of ClipScore indicating better concept inclusion as in the patch size case.

Table 7. Effect of τ on a subset of the ComposeLoRA testbed. Temperature positively improves ClipScore.

	$N = 2$	$N = 3$	Avg.
$\tau = 0.002$	0.340 ± 0.030	0.361 ± 0.022	0.351
$\tau = 1$	0.329 ± 0.029	0.359 ± 0.022	0.344

9. Qualitative Examples

In Figure 9 and 10, we observe several qualitative trends that reinforce the motivations and findings presented in the main paper. First, the source images—generated using a naïve text-only baseline frequently omit key elements, underscoring the need for LoRA-driven concept composition even in ostensibly simple scenarios, as discussed in Sec. 6.

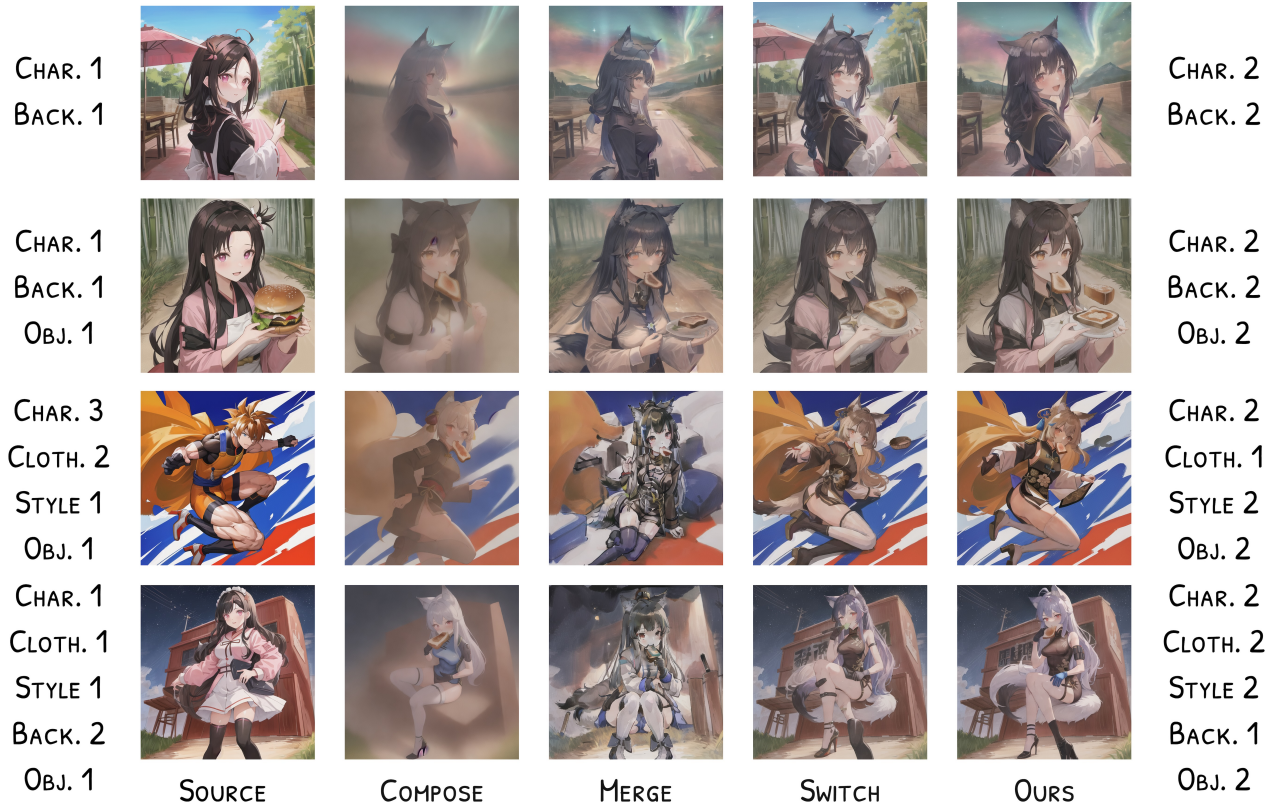


Figure 9. Examples of edits on the anime subset of the ComposeLoRA testbed for various N .

However, when editing these scenes, our method exhibits the lowest degree of concept erasure: all intended elements are consistently retained or added in the final outputs, aligning with the framework’s aim of preserving concept identity throughout editing. While all methods perform comparably for small compositions (*e.g.* $N = 2$), increasing the number of concepts and thus making the problem more challenging shows our methods advantage. More specifically, we see Merge introduces cumulative artefacts, whereas Switch progressively drops concepts as N grows. In contrast, our approach remains comparatively stable, maintaining coherent structure and concept fidelity even in more challenging multi-LoRA settings, reflecting the robustness of the unified Optimised DDS and compositional mechanism introduced in the main paper.

10. Qualitative Results

In addition to the results in Sec. 5.3, we provide a breakdown of GPTV evaluation win rates by subset of the ComposeLoRA testbed in Figure 11a and Figure 11. We also show detailed Image and Composition Quality scores for the two subsets in Tab. 8.

11. GPT-4V Evaluation Interface

To complement our quantitative metrics and human studies, we conduct a large-scale qualitative evaluation using GPT-4V, following and adapting the methodology of [41]. Unlike prior work focused on text-to-image generation, our task involves evaluating image editing quality. Therefore, we modify the evaluation prompt to reflect the specific goals of editing—namely, preserving source content while achieving target modifications. For each test case, GPT-4V is presented with: (a) two edited outputs (from our method and a baseline), and (b) a structured description of the source composition and the intended target composition.

GPT-4V is asked to evaluate the two edited images across two dimensions, namely Image Quality (*i.e.* assessing visual fidelity, absence of artefacts, and overall aesthetic) and Composition Quality (*i.e.* assessing how well the edit reflects the intended transformation while preserving identity and structure).

Each pairwise comparison is conducted twice with the image order reversed to mitigate positional bias. Scores are averaged across both runs. The evaluation prompt is detailed in Listing 1.



Figure 10. Examples of edits on the reality subset of the ComposeLoRA testbed for various N .

Table 8. Comparison of our Optimised DDS with concept composition against previous LoRA-composition methods, evaluated using GPT-4V. Our method achieves a total higher Image and Composition Quality scores.

	$N = 2$		$N = 3$		$N = 4$		$N = 5$		Total	
	Image Q.	Composition Q.	Image Q.	Composition Q.						
Merge	8.42	7.83	8.27	7.95	8.62	7.59	8.23	6.35	8.39	7.43
Switch	8.46	8.21	8.57	7.91	8.74	6.97	8.69	6.6	<u>8.62</u>	<u>7.42</u>
Composite	7.94	7.46	8.02	7.43	7.94	6.94	7.84	6.02	7.94	6.96
Ours	8.89	8.85	8.83	8.47	8.88	7.86	8.87	7.15	8.87	8.08

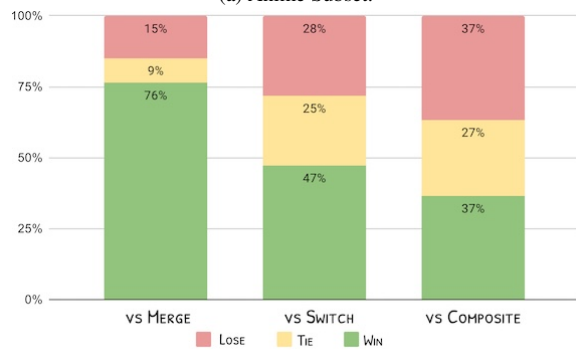
(a) Anime Subset

	$N = 2$		$N = 3$		$N = 4$		$N = 5$		Total	
	Image Q.	Composition Q.	Image Q.	Composition Q.						
Merge	7.56	7.94	7.38	7.45	7.56	6.89	7.33	6.5	7.46	7.20
Switch	8.74	8.37	8.7	8.23	8.39	7.16	8.1	7.0	8.48	7.69
Composite	8.75	8.65	8.73	8.44	8.73	8.02	8.67	7.9	<u>8.72</u>	<u>8.25</u>
Ours	8.87	8.81	8.78	8.5	8.74	8.21	8.85	8.11	8.81	8.41

(b) Reality Subset



(a) Anime Subset.



(b) Reality Subset.

Figure 11. **Comparison of our Optimised DDS with concept composition against previous LoRA-composition methods, evaluated using GPT-4V.** Our method achieves consistently higher pairwise win rates.

12. Human Evaluation

For the human qualitative evaluation, we asked three human experts to rank images produced by the four methods. For each combination, we provide a set of reference images and the output of the anonymised methods. Samples of the instructions and survey, as shown to human experts, are presented below. The Kendall's coefficient of concordance [16] is used as a metric of inter-annotator agreement for the ranking, with a value of 0.68 showing substantial agreement.

```
Image 2: Composition Quality: [score]/10,  
Image Quality: [score]/10
```

```
Based on the above guidelines, help me to  
conduct a step-by-step comparative  
evaluation of the given images. The  
scoring should follow two principles:  
1. Please evaluate critically.  
2. Try not to let the two models end in a  
tie on both dimensions.
```

Listing 1. GPT-4V Evaluation Prompt

```
I need assistance in evaluating image  
editing methods. You will see two  
images:  
  
1. Edited image from Method 1  
2. Edited image from Method 2  
  
SOURCE COMPOSITION:  
<source_elements>  
  
TARGET COMPOSITION (what the edited images  
should achieve):  
<target_elements>  
  
Please evaluate both edited images (Images  
1 and 2) on the following two  
dimensions:  
  
1. IMAGE QUALITY (0-10, 0.5 increments):  
- Deduct 3 points for each deformity (extra  
limbs, distorted faces, incorrect  
proportions)  
- Deduct 2 points for noticeable issues  
with texture, lighting, or color  
- Deduct 1 point for minor flaws or  
imperfections  
- Additional deductions can be made for any  
issues affecting the overall aesthetic  
or clarity of the image.  
  
2. COMPOSITION QUALITY (0-10, 0.5  
increments):  
- Deduct 3 points if any target element is  
missing or incorrectly depicted  
- Deduct 1 point for each missing feature  
within an element  
- Deduct 1 point for minor inconsistencies  
or lack of harmony  
- Additional deductions can be made for  
compositions that lack coherence,  
creativity, or realism.  
  
Please format the evaluation as follows:  
  
For Image 1:  
[Explanation of evaluation]  
  
For Image 2:  
[Explanation of evaluation]  
  
Scores:  
Image 1: Composition Quality: [score]/10,  
Image Quality: [score]/10
```

Image Editing Survey

Purpose

This evaluation aims to compare different *text-guided image editing methods* based on how well they integrate new or modified elements into an existing image.

You will be shown:

- A **source image**
- The **original text description** associated with the source image
- A **target text description** describing the desired edit or modification
- Four **generated target images** (in random order), each produced by a different image editing method

Your task is to **rank the four generated images from best (1) to worst (4)** according to two main criteria:

1. **Image Quality**
2. **Composition Quality**

1. Image Quality

Evaluate how visually realistic, clear, and aesthetically pleasing the image appears.

Consider the following:

- **Deformities:** Penalise images with distorted or unnatural body parts, incorrect object proportions, or extra/missing limbs.
- **Visual artefacts:** Deduct points for poor textures, inconsistent lighting, unnatural shadows, or colour mismatches.
- **Minor imperfections:** Small irregularities or blending issues should count as minor deductions.
- **Overall appeal:** Consider the general aesthetic coherence and clarity of the image—how “finished” and realistic it looks overall.

2. Composition Quality

Evaluate how accurately and harmoniously the image incorporates the requested changes from the target description.

Consider the following:

- **Missing or incorrect elements:** Deduct points if requested objects or features are absent or inaccurately depicted.
- **Incorrect details:** Penalise incorrect attributes within an element (e.g., wrong colour, size, or placement).
- **Consistency:** Check whether all parts of the image align naturally—objects should look properly integrated rather than pasted or out of place.
- **Faithfulness to the source:** The new image should maintain the original scene’s composition where appropriate, unless the edit specifically calls for major changes. Deduct points for unnecessary or drastic alterations unrelated to the edit request.
- **Adding elements:** If an element from the source description is missing in the source image, and the editing has corrected the omission, add points.

Ranking

For each set of images:

1. Review all four generated images carefully (click on the images to make the thumbnails larger).
2. Compare them in terms of **Image Quality** and **Composition Quality**.
3. Assign a **rank (1 = best, 4 = worst)** based on the overall balance of these two criteria.
4. If two images seem equally good, prioritise **Composition Quality** as the deciding factor.

Figure 12. Human Instructions for the Multi-Concept Editing task.



Son Goku, Burger -> Nezuko, Toast

1.  Method 4  
2.  Method 2  

3.  Method 1  

4.  Method 3  

Figure 13. Example Human Evaluation Interface.